Theoretical study of laser-induced surface excitations on a grating

Ki-Tung Lee and Thomas F. George
Department of Chemistry, University of Rochester, Rochester, New York 14627
(Received 23 July 1984)

Laser-induced surface excitations on a grating are studied in terms of the solutions to Maxwell's equations. A rigorous theory, derived originally for a lamellar grating, is used to study the resonance phenomenon for deep gratings. The generalization of the square-well grating to gratings of arbitrary shapes is examined numerically. A new diffraction anomaly is seen to occur when the grating depth is approximately equal to half of the wavelength of the incident laser radiation.

I. INTRODUCTION

It is well established that light impinging on a rough metallic surface may lead to resonant excitation of surface plasma oscillations, which play an important role in interesting surface phenomena, such as surface-enhanced Raman scattering[1,2] and laser-induced periodic pattern deposition.[3] In particular, the spatial oscillation of photochemically deposited metal films is identified as the fingerprint of the oscillation of a surface plasma wave (SPW). These surface waves are related or similar to those found in Wood's anomalies[4,5] or Brewster's waves,[6] which all satisfy the same mathematical equation but with media of different electric properties. Moreover, all of these waves have the same characteristics in that they propagate along the surface of a dielectric medium, with amplitudes decaying exponentially with increasing distance from the surface into the dielectrics and into the vacuum in contact with it. In the second quantization terminology, these surface waves are labeled as surface polaritons. Resonant excitation of these quasistationary modes can lead to orders of magnitude of enhancement of molecular processes occurring near or on the surface. (It has been suggested by Tsang and Kirtley[7] and later by Mill and Weber[8] that the maximum value of electric fields near gratings may be limited by grating-induced radiative damping.) Thus, a detailed understanding of the formation and the properties of these surface waves would be helpful in better understanding and controlling surface molecular rate processes and diagnosis of the properties of surfaces. (A comprehensive review of the diagnosis of surface properties can be found in Ref. 9.)

A general understanding of the physical properties of these surface waves has been reviewed by Fano,[5] and recent advances in research, both theoretically and experimentally, have been reviewed by Agranovich and Mills.[10] These quasistationary modes are controlled by the following elements: (a) the wavelength of the incident radiation, (b) the angle of incidence, (c) the geometry of the surface roughness, (d) the electric properties of the surface, and (e) the polarization.

One approach to the theory of surface plasma oscillations has been in terms of the collective motion of electrons in the solid.[11] It has been found, however, that the problem of resonant excitation of SPW can be treated more easily as an optical problem than as the collective motion of the electrons. In fact, both the problems of surface-enhanced Raman scattering[12] and laser-induced pattern deposition[3] have been examined by Rayleigh's perturbative diffraction theory.[13]

The formation of these evanescent waves originates a momentum transfer from the grating (roughness) to the impinging waves. Since the frequency of the impinging laser radiation is unaffected by the roughness, the modulus of the momentum of any wave must equal the one in the vacuum. Thus, momentum transfer by the roughness can only change the direction of momentum. This means that when the tangential component of the momentum of the diffractive wave,

$$k_{mt}=k_t+\frac{2\pi m}{d}\ , \tag{1}$$

(where k_t is the tangential component of the incident wave, d is the period of the grating, and m is an integer), is larger than the modulus of the incident momentum, k_0, then the normal component of the diffractive wave,

$$k_n=(k_0^2-k_{mt}^2)^{1/2}\ ,$$

becomes imaginary. This corresponds to evanescent waves travelling with momentum k_{mt} along the surface and exponentially damped in the normal direction. Moreover, if the geometry is chosen so certain kinematical conditions are met, the incident photon will resonantly couple to these surface polaritons.

The effect of the grating depth on the resonant conditions has been studied recently by Garcia[14] and Nevière and Reinisch.[15] While Garcia found that the intensities of the reflectivity and the diffraction beams have their minimum at resonance, but that the reflectivity becomes a maximum for a particular value of the grating depth, Nevière and Reinisch[15] pointed out that there exists an optimum value of the grating depth for which the electromagnetic (EM) resonance contribution to the enhancement of the nonlinear optical process is the greatest, and the optimization is achieved with very shallow modulation. More recently, Glass, Weber, and Mills,[16] utilizing the extinction theorem of Toigo, Marvin, Celli, and Hill,[17]

 ©1985 The American Physical Society

studied the grating-induced radiative damping of the surface polariton for grating profiles with various shapes and depths, and compared the results with those of perturbation theory. Good agreement was found for those systems investigated. All of the calculations mentioned above fall in the regime that the grating amplitude is much smaller than the incident wavelength. In this paper, we employ the square-well grating theory of Sheng, Stepleman, and Sanda,[18] which is based on the formalism of a stratified medium,[19] to study a new kind of resonance condition for a grating depth comparable to the incident wavelength.

Recently, various numerical techniques[20] have been developed for the solution of diffraction problems. Although most of these are rigorous in formulation, they exhibit various degrees of effectiveness in actual calculations. Very often numerical difficulties are found either when the grating depth becomes too large[21] or when the conductivity of the grating is large.[20] The square-well grating approach[18] has been demonstrated to be numerically stable even in the regime of good conductivity and also to work well for the case of a deep grating. However, the method is restricted to a lamellar grating. We have suggested a generalization of the square-well grating theory to gratings of arbitrary shape.[22] In this paper, the numerical applicability of this generalized theory is examined. Recently, the diffraction from gratings of arbitrary shape has attracted much attention. Moharan and Gaylord have applied their coupled-wave theory[23] to a multilayered grating formalism,[24] while Suratteau, Cadilhac, and Petit[25] formulated a "multistep lamellar grating" (MSLG) method by extending the work of Botten and coworkers.[26] The MSLG method, which has only been applied to lossless dielectrics, is believed to be closely related to the present work. In Sec. II, the theory of the square-well grating and its generalization to a multilayered grating is briefly reviewed. The results and discussion are given in Sec. III, and a summary is presented in Sec. IV.

II. THEORY

A. Square-well grating

The square-well grating formalism is based on a stratified medium model,[17] and a detailed account of the derivation can be found in a paper by Sheng, Stepleman, and Sanda.[18] Our main purpose in this part of Sec. II is to set up the notation for the generalization of the square-well grating to a multilayered grating.

Following Rayleigh's approach, the entire space is separated into three regions: the vacuum region (region I), the dielectric region (region III), and the corrugation region (region II). The geometry and the coordinate system of the lamellar grating are shown in Fig. 1. In regions I and III, the EM fields are expressed in terms of Rayleigh waves,

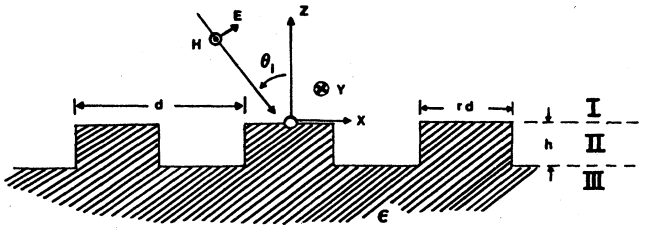

FIG. 1. Geometry and coordinate system for a p-wave incident on a square-well grating.

$$\Psi^{\mathrm{I}}=\exp\{ik_0[\sin(\theta_i)x-\cos(\theta_i)z]\}-\sum_{n=-\infty}^{\infty}R_n\exp\{ik_0[\gamma_n x+(1-\gamma_n^2)^{1/2}z]\} \tag{2}$$

and

$$\Psi^{\mathrm{III}}=\sum_{n=-\infty}^{\infty}T_n\exp\{ik_0[\gamma_n x-(\epsilon-\gamma_n^2)^{1/2}z]\}\ . \tag{3}$$

For p-wave scattering, Ψ is the y component of the magnetic vector, $k_0=2\pi/\lambda$ is the free-space wave vector of the incident laser radiation, ϵ is the dielectric constant of the grating, R_n and T_n are the amplitudes of the nth reflected and transmitted diffracted orders, θ_i is the angle of incidence, and

$$\gamma_n=\sin\theta_i+n\lambda/d\ , \tag{4}$$

where d is the period of the grating. (The square root with positive imaginary part will always be chosen in this paper.) The field in region II satisfies[16]

$$\frac{\partial^2\Psi^{\mathrm{II}}}{\partial z^2}+\frac{\partial^2\Psi^{\mathrm{II}}}{\partial x^2}+\epsilon(x)k_0^2\Psi^{\mathrm{II}}=\frac{\partial\Psi^{\mathrm{II}}}{\partial x}\frac{d}{dx}\ln[\epsilon(x)]\ , \tag{5}$$

where $\epsilon(x)=\epsilon$ for $|x-nd|\le rd/2$, and 1 otherwise (r is a number between 0 and 1). At this stage, the problem becomes identical to that of a periodically stratified medium with a piecewise constant ϵ.[17] Thus, the field in region II can be expressed in general as

$$\Psi^{\mathrm{II}}=\sum_l X_l(x)[A_l\exp(i\Lambda_l z)+B_l\exp(-i\Lambda_l z)]\ , \tag{6}$$

where Λ_l^2 are the eigenvalues satisfying the transcendental equation

$$\cos(k_0 d\sin\theta_i)+\cos(\beta_l rd)\cos[\alpha_l(1-r)d]+\frac{1}{2}\left[\epsilon\frac{\alpha_l}{\beta_l}+\frac{\beta_l}{\epsilon\alpha_l}\right]\sin(\beta_l rd)\sin[\alpha_l(1-r)d]=0\ , \tag{7}$$

and the associated eigenfunctions $X_l(x)$ are given by

$$X_l(x)=\begin{cases}\cos\left[\beta_l\left[x+\frac{rd}{2}\right]\right]+iV_0^l\frac{\epsilon k_0}{\beta_l}\sin\left[\beta_l\left[x+\frac{rd}{2}\right]\right], & |x|\le\frac{rd}{2}\\ U^l\cos\left[\alpha_l\left[x-\frac{rd}{2}\right]\right]+iV_1^l\frac{k_0}{\alpha_l}\sin\left[\alpha_l\left[x-\frac{rd}{2}\right]\right], & \frac{rd}{2}\le x\le\left[1-\frac{r}{2}\right]d\end{cases} \tag{8}$$

where $X_l(-rd/2)$ is normalized to 1, with

$$V_0^l=[\exp(ik_0d\sin\theta_i)-M_l]/N_l\ , \tag{9}$$

$$V_1^l=\frac{i}{k_0}\frac{\beta_l}{\epsilon}\sin(\beta_l rd)+V_0^l\cos(\beta_l rd)\ , \tag{10}$$

$$U^l=\cos(\beta_l rd)+iV_0^l\frac{\epsilon k_0}{\beta_l}\sin(\beta_l rd)\ , \tag{11}$$

$$M_l=\cos(\beta_l rd)\cos[\alpha_l(1-r)d]-\frac{\beta_l}{\epsilon\alpha_l}\sin[\alpha_l(1-r)d]\sin(\beta_l rd)\ , \tag{12}$$

$$N_l=ik_0\left[\frac{1}{\alpha_l}\cos(\beta_l rd)\sin[\alpha_l(1-r)d]+\frac{\epsilon}{\beta_l}\sin(\beta_l rd)\cos[\alpha_l(1-r)d]\right]\ , \tag{13}$$

$$\alpha_l=(k_0^2-\Lambda_l^2)^{1/2}\ , \tag{14}$$

$$\beta_l=(\epsilon k_0^2-\Lambda_l^2)^{1/2}\ . \tag{15}$$

The remaining task is to determine the expansion coefficients, R_n, T_n, A_l, and B_l, by matching the analytic solutions of Maxwell's equations at the boundaries; namely, the continuity of tangential E and H fields at $z=0$ and $z=-h$. This gives four simultaneous equations which are valid for all x:

$$\sum_n\exp(ik_0\gamma_n x_j)(\delta_{n0}-R_n)=\sum_l X_l(x_j)(A_l+B_l)\ , \tag{16}$$

$$\sum_l X_l(x_j)[A_l\exp(-i\Lambda_l h)+B_l\exp(i\Lambda_l h)]=\sum_n\exp\{ik_0[\gamma_n x_j+(\epsilon-\gamma_n^2)^{1/2}h]\}T_n\ , \tag{17}$$

$$\sum_n -ik_0[\cos(\theta_i)\delta_{n0}+(1-\gamma_n^2)^{1/2}R_n\exp(ik_0\gamma_n x_j)]=\sum_l i\frac{X_l}{\epsilon}(x_j)\Lambda_l(A_l-B_l)\ , \tag{18}$$

$$\sum_l\frac{X_l(x_j)}{\epsilon}i\Lambda_l[A_l\exp(-i\Lambda_l h)-B_l\exp(i\Lambda_l h)]=\frac{1}{\epsilon}\sum_n -ik_0(\epsilon-\gamma_n^2)^{1/2}T_n\times\exp[ik_0\gamma_n x_j+(\epsilon-\gamma_n^2)^{1/2}h]\ . \tag{19}$$

Employing the point matching method, we can rewrite Eqs. (16)—(19) in matrix notation as

$$\boldsymbol{D}-\boldsymbol{R}=\underline{\Gamma}^{-1}\underline{X}(\boldsymbol{A}+\boldsymbol{B})\ , \tag{20}$$

$$\underline{\Gamma}^{-1}\underline{X}(\underline{\Sigma}\boldsymbol{A}+\underline{\Sigma}^{-1}\boldsymbol{B})=\underline{\Delta}\boldsymbol{T}\ , \tag{21}$$

$$-\underline{\Pi}(\boldsymbol{R}+\boldsymbol{D})=\underline{\Gamma}^{-1}\underline{\Omega}(\boldsymbol{A}-\boldsymbol{B})\ , \tag{22}$$

$$\underline{\Gamma}^{-1}\underline{\Omega}(\underline{\Sigma}\boldsymbol{A}-\underline{\Sigma}^{-1}\boldsymbol{B})=-\underline{\xi}\underline{\Delta}\boldsymbol{T}\ , \tag{23}$$

where

$$\Gamma_{jn}=\exp(ik_0\gamma_n x_j)\ , \tag{24}$$

$$X_{jl}=X_l(x_j)\ , \tag{25}$$

$$\Omega_{jl}=\frac{\Lambda_l}{\epsilon}X_l(x_j)\ , \tag{26}$$

$$\Sigma_{jl}=\exp(-i\Lambda_l h)\delta_{jl}\ , \tag{27}$$

$$\Pi_{nj}=k_0(1-\gamma_n^2)^{1/2}\delta_{nj}\ , \tag{28}$$

$$\Delta_{nj}=\exp[ik_0(\epsilon-\gamma_n^2)^{1/2}h]\delta_{nj}\ , \tag{29}$$

$$\xi_{nj}=\frac{k_0}{\epsilon}(\epsilon-\gamma_n^2)^{1/2}\delta_{nj}\ . \tag{30}$$

$\boldsymbol{D}$ is defined as $\boldsymbol{D}_m=\delta_{m0}$. After some manipulation, we have the expressions for $\boldsymbol{R}$ and $\boldsymbol{T}$ in matrix form as

$$\boldsymbol{R}=(\underline{\Theta}-\underline{\Pi})^{-1}(\underline{\Theta}+\underline{\Pi})\boldsymbol{D} \tag{31}$$

with

$$\underline{\Theta}=-\{(\underline{\Gamma}^{-1}\underline{\Omega}+\underline{\xi}\underline{\Gamma}^{-1}\underline{X})\underline{\Sigma}+[(\underline{\Gamma}^{-1}\underline{\Omega}-\underline{\xi}\underline{\Gamma}^{-1}\underline{X})\underline{\Sigma}^{-1}]\underline{\Omega}^{-1}\underline{\Gamma}\}^{-1}\times[(\underline{\Gamma}^{-1}\underline{\Omega}+\underline{\xi}\underline{\Gamma}^{-1}\underline{X})\underline{\Sigma}-(\underline{\Gamma}^{-1}\underline{\Omega}-\underline{\xi}\underline{\Gamma}^{-1}\underline{X})\underline{\Sigma}^{-1}]\underline{X}^{-1}\underline{\Gamma} \tag{32}$$

and

TABLE I. Diffraction amplitudes of the first three orders for different number of layers in the square-well grating and for different ratios of the amplitude to the period.

		Numbers of layers		
	h/d	1	4	10
$\lvert R_0\rvert$	0.10	0.9712	0.9739	0.9739
	0.20	0.9551	0.9588	0.9588
	0.28	0.2367	0.1969	0.1969
$\lvert R_1\rvert$	0.10	0.1744	0.1567	0.1567
	0.20	0.2298	0.2110	0.2110
	0.28	0.8551	0.8478	0.8478
$\lvert R_2\rvert$	0.10	0.0251	0.0310	0.0310
	0.20	0.0411	0.0430	0.0430
	0.28	0.2775	0.2055	0.2054

$$\boldsymbol{T}=2\underline{\Delta}^{-1}\underline{K}^{-1}\underline{X}^{-1}\underline{\Gamma}(\boldsymbol{D}-\boldsymbol{R}) , \tag{33}$$

where

$$\underline{K}=\underline{\Sigma}^{-1}(\underline{X}^{-1}\underline{\Gamma}-\underline{\Omega}^{-1}\underline{\Gamma}\underline{\xi})+\underline{\Sigma}(\underline{X}^{-1}\underline{\Gamma}+\underline{\Omega}^{-1}\underline{\Gamma}\underline{\xi}) . \tag{34}$$

For $h=0$, both $\underline{\Sigma}$ and $\underline{\Delta}$ reduce to identity matrices. In this case, $\underline{\Theta}$ becomes $-\underline{\xi}$, which directly implies

$$\boldsymbol{R}=(\underline{\xi}+\underline{\Pi})^{-1}(\underline{\xi}-\underline{\Pi})\boldsymbol{D} \tag{35}$$

and

$$\boldsymbol{T}=\boldsymbol{D}-\boldsymbol{R} , \tag{36}$$

which are the correct expressions for flat surfaces. In the case of a very deep grating, $h\rightarrow\infty$, and for Λ_l with an imaginary part of any size, $\underline{\Sigma}_{ll}\rightarrow\infty$, then $\underline{\Theta}$ can be reduced to a simple form, $-\underline{\Omega}\underline{X}^{-1}$, and the partial field $[\underline{\Delta}\boldsymbol{T}]_l$ goes to zero. The resonant excitation conditions are given mathematically by the zero's of the expression $(\underline{\Theta}+\underline{\Pi})^{-1}(\underline{\Theta}-\underline{\Pi})$ and physically are governed by the five parameters given in Sec. I. Although these parameters have different degrees of importance in the control of the resonant excitation of the surface plasma oscillations, one can, with appropriate choice of these five parameters, engineer some interesting surface phenomena. Here, we focus on how the depth of the square-well grating may introduce such phenomena.

B. Multilayered grating

We now extend the square-well grating formalism to a multilayered grating theory which can model gratings of arbitrary shape. This involves the extension of the concept of a periodic stratified medium to a two-dimensional scheme. A schematic diagram of the multilayered grating is illustrated in Fig. 2, where region II is divided into subregions. In each subregion, the electromagnetic field is expressed as in Eq. (6),

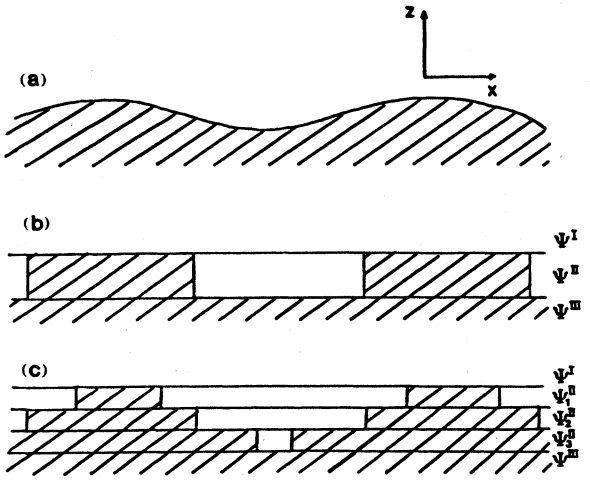

FIG. 2. (a) Sinusoidal grating. The cross-hatched area represents the metal. (b) Square-well grating showing a separation into three layers, one of which is periodic in the x direction and two of which are uniform. (c) Generalization of the square-well grating in which there are three periodic layers.

$$\Psi_m^{\mathrm{II}}=\sum_l X_l^m(x)[A_l^m\exp(i\Lambda_l^m z)+B_l^m\exp(-i\Lambda_l^m z)] , \tag{37}$$

where m is the layer index. The characteristic equation of each layer is the same as Eq. (7). However, layers differ from each other by different values of r, which is a measure of the amount of metal within a grating period. Following the methodology of the square-well grating, we match the fields at the boundaries of each region and subregion. Hence, we have

$$\underline{\Gamma}^{-1}\underline{X}_0(\boldsymbol{A}_0+\boldsymbol{B}_0)=\boldsymbol{D}-\boldsymbol{R} , \tag{38}$$

$$\underline{\Gamma}^{-1}\underline{X}_n(\underline{\Sigma}_{n,n+1}\underline{A}_n+\underline{\Sigma}_{n,n+1}^{-1}\boldsymbol{B}_n)=\underline{\Delta}\boldsymbol{T} , \tag{39}$$

$$\underline{\Gamma}^{-1}\underline{\Omega}_0(\boldsymbol{A}_0-\boldsymbol{B}_0)=-\underline{\Pi}(\boldsymbol{D}+\boldsymbol{R}) , \tag{40}$$

$$\underline{\Gamma}^{-1}\underline{\Omega}_n(\underline{\Sigma}_{n,n+1}\boldsymbol{A}_n-\underline{\Sigma}_{n,n+1}^{-1}\boldsymbol{B}_n)=-\underline{\xi}\underline{\Delta}\boldsymbol{T} , \tag{41}$$

$$\underline{X}_{m-1}(\underline{\Sigma}_{m-1,m}\boldsymbol{A}_{m-1}+\underline{\Sigma}_{m-1,m}^{-1}\boldsymbol{B}_{m-1})=\underline{X}_{m+1}(\underline{\Sigma}_{m,m}\boldsymbol{A}_m+\underline{\Sigma}_{m,m}^{-1}\boldsymbol{B}_m) , \tag{42}$$

$$\underline{\Omega}_{m-1}(\underline{\Sigma}_{m-1,m}\boldsymbol{A}_{m-1}-\underline{\Sigma}_{m-1,m}^{-1}\boldsymbol{B}_{m-1})=\underline{\Omega}_{m+1}(\underline{\Sigma}_{m,m}\boldsymbol{A}_m-\underline{\Sigma}_{m,m}^{-1}\boldsymbol{B}_m) , \tag{43}$$

with $m=1,\ldots,n$, and the grating has $n+1$ layers with a thickness of h. The elements of the $\underline{\Sigma}$ matrix are given as

$$(\underline{\Sigma}_{u,v})_{p,q}=\exp(-i\Lambda_p^u vh)\delta_{pq} . \tag{44}$$

All other matrices are defined as in Sec. II A but with a subregion index. It is trivial to generalize the formalism to treat a different thickness for each layer. For simplicity, we choose each layer to have the same thickness.

In order to find expressions for $\boldsymbol{R}$ and $\boldsymbol{T}$, we construct the two supermatrix equations,

$$\begin{bmatrix}\underline{\Gamma}^{-1}\underline{X}_0 & \underline{\Gamma}^{-1}\underline{X}_0\\ \underline{\Gamma}^{-1}\underline{\Omega}_0 & -\underline{\Gamma}^{-1}\underline{\Omega}_0\end{bmatrix}\begin{bmatrix}\boldsymbol{A}_0\\ \boldsymbol{B}_0\end{bmatrix}=\begin{bmatrix}\boldsymbol{D}-\boldsymbol{R}\\ -\underline{\Pi}(\boldsymbol{D}+\boldsymbol{R})\end{bmatrix} \tag{45}$$

and

$$\begin{bmatrix}\underline{\Gamma}^{-1}\underline{X}_n\underline{\Sigma}_{n,n+1} & \underline{\Gamma}^{-1}\underline{X}_n\underline{\Sigma}_{n,n+1}^{-1}\\ \underline{\Gamma}^{-1}\underline{\Omega}_n\underline{\Sigma}_{n,n+1} & -\underline{\Gamma}^{-1}\underline{\Omega}_n\underline{\Sigma}_{n,n+1}^{-1}\end{bmatrix}\begin{bmatrix}\boldsymbol{A}_n\\ \boldsymbol{B}_n\end{bmatrix}=\begin{bmatrix}\underline{\Delta}\boldsymbol{T}\\ -\underline{\xi}\underline{\Delta}\boldsymbol{T}\end{bmatrix} . \tag{46}$$

We notice that the $\boldsymbol{A}$'s and $\boldsymbol{B}$'s are related by the recursive relationship

$$\begin{bmatrix}\underline{\Sigma}_{n,n} & \underline{\Sigma}_{n,n}^{-1}\\ \underline{\Sigma}_{n,n} & -\underline{\Sigma}_{n,n}^{-1}\end{bmatrix}\begin{bmatrix}\boldsymbol{A}_n\\ \boldsymbol{B}_n\end{bmatrix}=\begin{bmatrix}\underline{X}_n^{-1}\underline{X}_{n-1}\underline{\Sigma}_{n-1,n} & \underline{X}_n^{-1}\underline{X}_{n-1}\underline{\Sigma}_{n-1,n}^{-1}\\ \underline{\Omega}_n^{-1}\underline{\Omega}_{n-1}\underline{\Sigma}_{n-1,n} & -\underline{\Omega}_n^{-1}\underline{\Omega}_{n-1}\underline{\Sigma}_{n-1,n}^{-1}\end{bmatrix}\begin{bmatrix}\boldsymbol{A}_{n-1}\\ \boldsymbol{B}_{n-1}\end{bmatrix} . \tag{47}$$

Hence, we have

$$\begin{bmatrix}\boldsymbol{A}_n\\ \boldsymbol{B}_n\end{bmatrix}=\begin{bmatrix}a & b\\ c & d\end{bmatrix}\begin{bmatrix}\boldsymbol{A}_0\\ \boldsymbol{B}_0\end{bmatrix} , \tag{48}$$

where

$$\begin{bmatrix} a & b \\ c & d \end{bmatrix} = \frac{(-1)^n}{2^n} \begin{bmatrix} \underline{\Sigma}_{nn}^{-1} & \underline{\Sigma}_{nn}^{-1} \\ \underline{\Sigma}_{nn} & -\underline{\Sigma}_{nn} \end{bmatrix} \begin{bmatrix} \underline{X}_n^{-1}\underline{X}_{n-1}\underline{\Sigma}_{n-1,n} & \underline{X}_n^{-1}\underline{X}_{n-1}\underline{\Sigma}_{n-1,n}^{-1} \\ \underline{\Omega}_n^{-1}\underline{\Omega}_{n-1}\underline{\Sigma}_{n-1,n} & -\underline{\Omega}_n^{-1}\underline{\Omega}_n\underline{\Sigma}_{n-1,n}^{-1} \end{bmatrix}$$

$$\times \begin{bmatrix} \underline{\Sigma}_{n-1,n-1}^{-1} & \underline{\Sigma}_{n-1,n-1}^{-1} \\ \underline{\Sigma}_{n-1,n-1} & -\underline{\Sigma}_{n-1,n-1} \end{bmatrix} \begin{bmatrix} \underline{X}_{n-1}^{-1}\underline{X}_{n-2}\underline{\Sigma}_{n-2,n-1} & \underline{X}_{n-1}^{-1}\underline{X}_{n-2}\underline{\Sigma}_{n-2,n-1} \\ \underline{\Omega}_{n-1}^{-1}\underline{\Omega}_{n-2}\underline{\Sigma}_{n-2,n-1} & -\underline{\Omega}_{n-1}^{-1}\underline{\Omega}_{n-2}\underline{\Sigma}_{n-2,n-1} \end{bmatrix}$$

$$\times \cdots \times \begin{bmatrix} \underline{X}_1^{-1}\underline{X}_0\underline{\Sigma}_{0,1} & \underline{X}_1^{-1}\underline{X}_0\underline{\Sigma}_{0,1}^{1} \\ \underline{\Omega}_1^{-1}\underline{\Omega}_0\underline{\Sigma}_{0,1} & -\underline{\Omega}_1\underline{\Omega}_0\underline{\Sigma}_{0,1}^{-1} \end{bmatrix} . \tag{49}$$

Substituting Eqs. (46) and (48) into (45), we have

$$\begin{bmatrix} \underline{K} & \underline{L} \\ \underline{M} & \underline{N} \end{bmatrix} \begin{bmatrix} D-R \\ -\underline{\Pi}(D+R) \end{bmatrix} = \begin{bmatrix} \underline{\Delta}T \\ -\underline{\xi}\underline{\Delta}T \end{bmatrix} , \tag{50}$$

where

$$\begin{bmatrix} \underline{K} & \underline{L} \\ \underline{M} & \underline{N} \end{bmatrix} = \frac{1}{2} \begin{bmatrix} \underline{\Gamma}^{-1}\underline{X}_n\underline{\Sigma}_{n,n+1} & \underline{\Gamma}^{-1}\underline{X}_n\underline{\Sigma}_{n,n+1}^{-1} \\ \underline{\Gamma}^{-1}\underline{\Omega}_n\underline{\Sigma}_{n,n+1} & -\underline{\Gamma}^{-1}\underline{\Omega}_n\underline{\Sigma}_{n,n+1}^{-1} \end{bmatrix}$$

$$\times \begin{bmatrix} a & b \\ c & d \end{bmatrix} \begin{bmatrix} \underline{X}_0^{-1}\underline{\Gamma} & \underline{\Omega}_0^{-1}\underline{\Gamma} \\ \underline{X}_0^{-1}\underline{\Gamma} & -\underline{\Omega}_0^{-1}\underline{\Gamma} \end{bmatrix} . \tag{51}$$

The expressions for $\boldsymbol{R}$ and $\boldsymbol{T}$ are then given as

$$\boldsymbol{R} = [(\underline{\xi}\underline{K}+\underline{M})+(\underline{\xi}\underline{L}+\underline{N})\underline{\Pi})]^{-1} \times [(\underline{\xi}\underline{K}+\underline{M})-(\underline{\xi}\underline{L}+\underline{N})\underline{\Pi}]D \tag{52}$$

and

$$\boldsymbol{T} = \underline{\Delta}^{-1}(\underline{L}^{-1}+\underline{N}^{-1}\underline{\xi})^{-1}(\underline{L}^{-1}\underline{K}-\underline{N}^{-1}\underline{M})(D-R) . \tag{53}$$

Equations (52) and (53) are now all we require to calculate the fields at the peaks and troughs of the grating.

III. RESULTS AND DISCUSSION

A. Square-well grating

Numerical calculations have been carried out for a diffraction system with an incident wavelength of $\lambda = 6471$ Å, a grating periodicity of $d = 1$ μm, and the incident angle fixed perpendicular to the grating surface. Under this configuration, the (first-order) perturbation theory predicts no resonant excitation. The diffraction amplitudes are computed as a function of the groove depth for a silver grating with the dielectric constant, $\epsilon = -17.42 + 0.58i$, chosen to fit experimental data.[18] Results are plotted in Fig. 3 for the three lowest diffraction orders. Since the angle of emergence for R_2 is complex, R_2 is a surface wave. As shown in Fig. 3, for a ratio of the grating amplitude to the period of 0.283, the reflected beam is at its minimum, while the first- and second-order diffraction beams are at their maxima.

To understand this behavior, one can draw an analogy to resonant scattering theory, in particular, the bound-continuum interaction problem,[27] where a quasibound state plays the role as a coupling between the bound state and the continuum states. At the resonant energy, an interference structure, which is due to a competition between two equally possible pathways, occurs in the cross

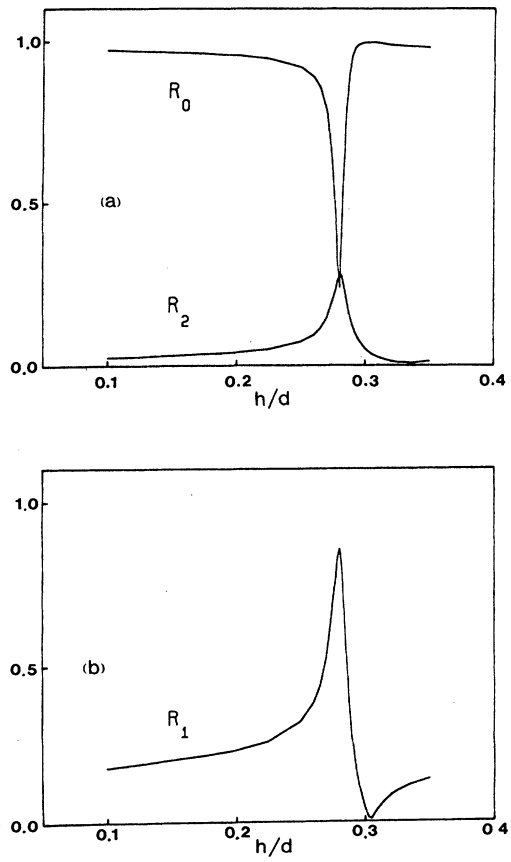

FIG. 3. (a) Magnitudes of the zeroth- and second-order diffraction amplitudes plotted as a function of the ratio of the amplitude to the period ($d = 1000$ nm). (b) Magnitude of the first-order amplitude plotted as a function of the ratio of the amplitude to the period ($d = 1000$ nm), with $r = 0.5$.

TABLE II. Average field intensity at the peak and at the trough, as a function of the ratio of the grating amplitude to the period, for a three-layered grating with a profile as described in Fig. 2(c).

h/d	$\lvert\bar{\Psi}\rvert^2$ peak	$\lvert\bar{\Psi}\rvert^2$ trough
0.003	1.020	0.137
0.006	1.057	0.923(−1)
0.009	1.089	0.646(−1)
0.012	1.117	0.469(−1)
0.015	1.114	0.352(−1)
0.018	1.168	0.270(−1)
0.021	1.191	0.212(−1)
0.024	1.211	0.170(−1)
0.027	1.230	0.139(−1)
0.030	1.248	0.115(−1)
0.060	1.363	0.288(−2)
0.090	1.419	0.112(−2)
0.120	1.452	0.515(−2)
0.150	1.473	0.250(−3)
0.180	1.491	0.120(−3)

section. In the present case, the grating roughness serves as the coupling between the incident wave and the surface waves. At an optimum depth, the incident wave couples strongly with the surface waves. Thus, the resonance occurs. Moreover, the direct and indirect diffraction channels interfere with each other and construct the Fano-type interference structure in the first-order diffraction beam. The resonance arises when the cavity (the groove) has a depth of approximately half of the incident wavelength, which is analogous to the case of acoustic resonances in an open-ended organ pipe occurring when $(n+\frac{1}{2})\lambda$ equals the length of the pipe, where n is an integer. In the present case, we believe that the deviation from precisely a half is partially due to the fact that the delectric constant of the Ag grating has a finite nonzero imaginary part, such that the damping mechanism leads to a width as well as a shift in the resonant condition.[28] A calculation similar to the one of Glass, Weber, and Mill[16] would be helpful to further understand these frequency shifts and damping rates, which is being carried out in our laboratory. As far as we know, this Fano-type interference resonance phenomenon by diffraction from a grating has never been reported before.

B. Layered grating

In this part, we discuss the numerical applicability of the formalism derived in Sec. II B. We test the formalism by separating the square-well grating into a fictitious layered grating, as shown in Fig. 4. We then apply the multilayered grating formalism to this fictitious layered grating for four and ten layers. Numerical results are compared with those of the square-well grating in Table I for the first three orders of diffraction beams at various grating depth. First, the results for four layers are almost identical with those for ten layers. This implies that the method is stable for a multilayered configuration, which is important for modeling gratings of different shapes. Second, the layered grating results are, in general, in good

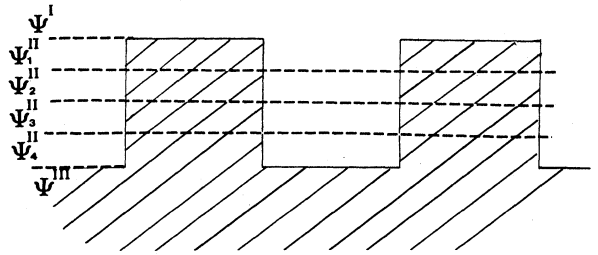

FIG. 4. Schematic diagram for a fictitious square-well layered grating.

agreement with the square-well grating results, except near resonance, especially when the numbers are small. We believe this discrepancy is due to the degree of accuracy of the matrix inversion, since in the layered grating formalism one needs to invert matrices which are twice the size of those in the square-well grating approach. These matrices appear to become singular whenever the scattering is at resonance. Moreover, we find that the expression for T_n, Eq. (53), is unstable, especially when the grating amplitude is large. This also occurs in the square-well case when T_n takes the form of Eq. (53). A more stable expression might be achieved by first evaluating the A and B coefficients.

We now turn to a calculation on a three-layered grating. The surface profile has a structure somewhat between a sawtooth grating and a sinusoidal grating, as shown in Fig. 2(c). We have calculated the average field at the peak and at the trough of the grating as a function of the grating depth, with the same scattering parameters as above with values of r (see Fig. 1) as 0.1, 0.3, and 0.5. The results are presented in Table II. We find that T_n begins to exhibit unstable behavior as the ratio of the grating amplitude to the period reaches 0.2. Otherwise, both fields are convergent and stable.

The difficulties in this layered grating approach arise from the evaluation of the nonlinear eigenvalues of Eq. (7). As mentioned by Sheng, Stepleman, and Sanda,[18] eigenfunctions whose eigenvalues form complex conjugate pairs should not be separated. While truncation of the matrices is inevitable and the number of eigenfunctions used for each layer should be equal, a tremendous amount of manual labor and computer time are required to match these two criteria. This is a potential problem in modeling a realistic profile.

IV. SUMMARY

A new diffraction anomaly is seen to occur when the grating amplitude is approximately equal to half of the incident wavelength. When the resonance condition is met, the radiated energy (the scattered light) changes its "preferred" direction, and at the same time surface waves are excited.

A new multilayered grating method has been formulated to model grating profiles of arbitrary shape. The field at the peak remains stable as the grating depth increases, while the field at the trough (inside the metal) does not. Difficulties are found in choosing an optimum basis set.

A supercomputer would be helpful for applying this multilayered grating formalism to model specific surface profiles.

ACKNOWLEDGMENTS

This research was supported by the Office of Naval Research and the Air Force of Scientific Research (AFSC), United States Air Force, under Grant No. AFOSR-82-0046. One of us (T.F.G.) acknowledges the Camille and Henry Dreyfus Foundation for support. We acknowledge helpful conversations with Michael Hutchinson and K. C. Liu.

[1]E. Burstein, C. Y. Chen, and S. Lundqvist, in *Light Scattering in Solids,* edited by J. L. Birman, H. Z. Cummins, and K. K. Rebane (Plenum, New York, 1979), p. 479.

[2]For a comprehensive review, see *Surface-Enhanced Raman Scattering,* edited by R. K. Chang and T. E. Furtak (Plenum, New York, 1981).

[3]S. R. J. Brueck and D. J. Ehrlich, Phys. Rev. Lett. **48**, 1678 (1982).

[4]R. W. Wood, Philos. Mag. **4**, 393 (1902); **23**, 310 (1912); Phys. Rev. **48**, 928 (1935).

[5]U. Fano, J. Opt. Soc. Am. **31**, 213 (1941).

[6]M. C. Hutley and D. Maystre, Opt. Commun. **19**, 431 (1976); D. Maystre and R. Petit, *ibid.* **17**, 196 (1976).

[7]J. C. Tsang, J. R. Kirtley, and T. N. Theis, Solid State Commun. **35**, 667 (1980).

[8]D. L. Mills and M. Weber, Phys. Rev. B **26**, 1075 (1982).

[9]For example, see *Surfaces Studies with Lasers,* edited by F. R. Aussanegg, A. Leitner, and M. E. Lippitsch (Springer, New York, 1983).

[10]A. A. Maradudin, in *Surface Polaritons,* edited by V. M. Agranovich and D. L. Mills (North-Holland, New York, 1982), p. 405.

[11]R. H. Ritchie, Surf. Sci. **34**, 1 (1973), and references therein.

[12]S. S. Jha, J. R. Kirtley, and J. C. Tsang, Phys. Rev. B **22**, 3973 (1980).

[13]Lord Rayleigh, Proc. R. Soc. London, Ser. A **79**, 399 (1907).

[14]N. Garcia, Opt. Commun. **45**, 307 (1983).

[15]M. Nevière and R. Reinisch, Phys. Rev. B **26**, 5403 (1982).

[16]N. E. Glass, M. Weber, and D. L. Mills, Phys. Rev. B **29**, 6548 (1984).

[17]F. Toigo, A. Marvin, C. Celli, and N. R. Hill, Phys. Rev. B **15**, 5618 (1977).

[18]Ping Sheng, R. S. Stepleman, and P. N. Sanda, Phys. Rev. B **26**, 2907 (1982).

[19]M. Born and E. Wolf, *Principles of Optics,* 6th ed. (Pergamon, New York, 1983), pp. 51—70.

[20]For example, see *Electromagnetic Theory of Diffraction Gratings,* edited by R. Petit (Springer, New York, 1980).

[21]N. Garcia, V. Celli, and N. R. Hill, Phys. Rev. B **18**, 5184 (1978).

[22]M. Hutchinson, K. T. Lee, W. C. Murphy, A. C. Beri, and T. F. George, in *Laser-Controlled Chemical Processing of Surfaces,* edited by A. W. Johnson, D. J. Ehrlich, and H. R. Schlossberg (Elsevier, New York, in press); Mater. Res. Soc. Symp. Proc. **29**, 389 (1984).

[23]M. G. Moharan and T. K. Gaylord, J. Opt. Soc. Am. **71**, 811 (1981).

[24]M. G. Moharan and T. K. Gaylord, J. Opt. Soc. Am. **72**, 1385 (1982).

[25]J. Y. Suratteau, M. Cadilhac, and R. Petit, J. Opt. (Paris) **14**, 273 (1983).

[26]L. C. Botten, M. S. Craig, R. C. McPhedran, J. L. Adams, and J. R. Andrewartha, Opt. Acta **28**, 413 (1981); **28**, 1087 (1981).

[27]U. Fano, Phys. Rev. **124**, 1866 (1961).

[28]J. D. Jackson, *Classical Electrodynamics,* 2nd ed. (Wiley, New York, 1975), p. 356.